Accepted Manuscript

Interannual variability of the early summer circulation around the Balearic Islands: driving factors and potential effects on the marine ecosystem

R. Balbín, J.L. López-Jurado, M.M. Flexas, P. Reglero, P. Vélez-Velchí, C. González-Pola, J.M. Rodríguez, A. García, F. Alemany

Interannual variability of the early summer circulation around the Balearic Islands: driving factors and potential effects on the marine ecosystem.

July 16, 2013

R. Balbín[a], J.L. López-Jurado[a], M.M. Flexas[e], P. Reglero[a], P. Vélez-Velchí[c], C. González-Pola[b], J.M. Rodríguez[b], A. García[d], F. Alemany[a]

[a]Instituto Español de Oceanografía, Centro Oceanográfico de Baleares, Muelle de Poniente s/n, 07015, Palma de Mallorca, Spain

[b]Instituto Español de Oceanografía, Centro Oceanográfico de Santander, Spain

[c]Instituto Español de Oceanografía, Centro Oceanográfico de Canarias, Spain

[d]Instituto Español de Oceanografía, Centro Oceanográfico de Málaga, Spain

[e]Jet Propulsion Laboratory, California Institute of Technology, 4800 Oak Grove Drive, Pasadena, CA91109, USA

Email Address:rosa.balbin@ba.ieo.es

Abstract

Six summer surveys conducted from 2001 to 2005 and in 2012 by the Spanish Institute of Oceanography (IEO) reveal that the hydrographic early summer scenarios around the Balearic Islands are related to the winter atmospheric forcing in the northwestern Mediterranean Sea. The Balearic Islands (western Mediterranean Sea) lie at the transition between the southern, fresher, newly arrived Atlantic Waters (AW) and the northern, saltier, resident AW. The meridional position of the salinity driven oceanic density front separating the new from the resident AW is determined by the presence/absence of Western Intermediate Water (WIW) in the Mallorca and Ibiza channels. When WIW is present in the channels, the oceanic density front is found either at the south of the islands, or along the Emil Boudot escarpment. In contrast, when WIW is absent, new AW progresses northwards crossing the Ibiza channel and/or the Mallorca channel. In this later scenario, the oceanic density front is closer to the Balearic Islands. A good correspondence exists between standardized winter air temperature anomaly in the Gulf ofLions and the presence of WIW in the channels. We discuss the use of a regional climatic index based on these parameters to forecast in a first-order approach the position of the oceanic front, as it is expected to have high impact on the regional marine ecosystem.

Keywords

Ocean circulation • oceanic fronts • water masses • Western Mediterranean Sea • Balearic Sea • regional climatic index

1. Introduction

The circulation in the Mediterranean Sea follows a cyclonic path along the continental slope (e.g. [27]). The inflow of Atlantic Waters (AW) through the Gibraltar strait extends across the Alboran Sea and follows the North African coast, configuring the Algerian Current

(AC). In the northwestern Mediterranean, at the Ligurian sub-basin, the AW flowing from the Algerian sub-basin joins to that coming from the Tyrrhenian Sea [5] forming the Northern Current (NC), which flows along the continental slope (Fig. 1A). When it arrives to the Balearic sub-basin a branch of this current flows northeastward along the northern slope of the Balearic Islands, giving rise to the Balearic Current (BC) [40,17].

Two water masses are found at intermediate depths: the Levantine Intermediate Water (LIW), formed at the Eastern Mediterranean Sea, and the Western Intermediate Water (WIW), formed in winter over the continental shelf and the slope (e.g. [45]). Western Mediterranean Deep Water (WMDW), is formed during deep winter convection events in the Gulf of Lions and the Ligurian Sea [26] and cascading [12,36].

WIW is transported by the NC into the Gulf of Valencia and the Ibiza channel between the end of winter and beginning of spring; however, it is not found at the Balearic channels every year. Table 1 resumes the salinity, S, and potential temperature, θ, that characterize the different water masses and their values in the area of study [24]. The saltier and colder surface water that has stayed longer in the Mediterranean will be denoted as resident AW (S > 37.5) and the fresher and warmer water recently arrived through the Strait of Gibraltar will be denoted as new or recent AW (S < 37.5).

At the end of the winter the southward transport through the channels decreases [15]. This allows the northward progress of recent AW across the Balearic channels during summer [34]. The confluence of new AW with resident AW generate salinity driven oceanic fronts that will be denoted as oceanic fronts from now on.

The presence of WIW at the topographically complex Balearic channels can induce the formation of mesoscale structures able to disrupt the local circulation [33,34].

Using a primitive equation model [32] find that the accumulation of WIW to the north of the Ibiza Channel in spring has a dramatic effect on the circulation and on the water exchange through the channels. They refer to WIW anticycloniceddies as "weddies" and find out they are the main factor leading to a reduction of the southward circulation through the Ibiza Channel. Those anticyclonic "weddies" induce an important branching of the NC, which is partly redirected toward the Balearic slope, reinforcing the BC. The mesoscale regional IDEA index [28] has satisfactorily characterized the presence or absence of WIW in the Balearic channels during spring and summer, making use of the data on the atmospheric forcing in the Gulf of Lions during the previous winter.

Marine ecosystems respond to the variability on the position of oceanic fronts and eddies (e.g. [22], and references therein). Fronts and eddies are places where the mechanical energy of the physical system is accessible for augmenting the trophic energy available to biological organisms [8]. Such habitats, though small in areal extent, may contribute disproportionately and importantly to regional productivity, nutrient cycling, carbon fluxes and trophic ecology [22]. These processes are also observed in the Balearic Sea (e.g. [35]) where mesoscale structures determinethe interannual differences in the spatial patterns of the meroplanktonic communities [2,44]. The locations of the fronts determine the interannual variability of the spawning habitat of large pelagic predators (e.g. bluefin tuna and albacore [37]). Fronts and eddies also play a major role in determining genetic connectivity and geographic fragmentation of fish species populations [42].

The goal of this paper is to examine the possibility of predicting qualitatively the location of the oceanic front separating new AW from resident AW at the beginning of summer using the mesoscale regional climatic IDEA index. The results might provide a tool useful to understand the influence of mesoscale structures on the ecosystems around the Balearic Islands, based on atmospheric conditions in the previous winter.

With this purpose, available data and the methods used for the analysis are presented in first place. Then, the hydrographical scenarios are described for the different surveys and the

presence or absence of WIW in the channels is illustrated. After that we discuss the dependence of the position of the oceanic front on WIW absence/presence on the channels, the use of the IDEA index to forecast the WIW presence on the channels, the implications that the front position has on the biology and the implications of predicting frontal positions using winter atmospheric forcing on understanding the biological systems. Finally, the conclusions are summarized.

2. Data and Methodology

Six summer surveys were carried out from 2001 to 2005 and 2012 (Table 2). They will be referred as Tunibal surveys. Hydrographic stations were 10 nmi apart (approximately 18.5 km). Such spatial resolution allows to resolve the typical regional mesoscale structures, which range from 50 km to 100 km [34]. Figure 1B shows the grid of Atame-0612 as an example of Tunibal standard sampling stations.

Conductivity, temperature and pressure (CTD) data from SeaBird 911+ and SeaBird 25 were obtained from surface to 350 m. Every two hydrographic stations (every 20 nmi) measurements were extended down to 600 m for dynamic height calculations. Hydrographic parameters (salinity, S; potential temperature, θ; potential density anomaly, σ_θ) were processed using the Sea-Bird Electronics Data Processing routines. Salinity was calibrated using IAPSO standard seawater and a Guildline 8400A salinometer. Temperature and salinity can be considered accurate within 0.005 °C and 0.003 units, respectively. Data at each station was processed at their original sampling frequency and averaged to get 1 m of vertical resolutionfor analysis.

Horizontal hydrodynamic fields were objectively analyzed onto a 3 × 3 nmi (approximately 5.5 × 5.5 km) regular grid by using minimum error variance methods [11]. An isotropic Gaussian spatial correlation function wasassumed for the anomaly spatial correlation, with a characteristic correlation scale of 18 nmi (approximately 33 km).

The climatological long term rms variability was set to 0.5. The noise-to-signal rms error was set at 0.1. Interpolated fields with rms error above 0.2 were disregarded.

Dynamic height was calculated by vertical integration of the specific volume, using 600 m as the level of no motion [35]. At shallow stations, or when data was recorded only down to 350 m, the density anomaly of the closest station (closer than 15 nmi) was assigned at the lower recorded level. Geostrophic velocities were obtained by the first-derivative of the dynamic height profiles objectively analyzed onto the 3 nmi × 3 nmi regular grid.

Satellite-derived Sea Surface Height (SSH) was obtained by calculating a Map of Absolute Dynamic Topography (MADT) as MADT=MDT+MSLA. Mean Dynamic Topography (MDT) was calculated by [38] and is available at MyOcean [7]. Map of Sea Level Anomaly (MSLA) was obtained from AVISO (Delay Time data) that provides data with a resolution of $1/8°$ and one week temporal resolution [6]. Geostrophic velocities were calculated from the first-derivative of the SSH between adjacent points.

During summer the surface heating is very intense and the satellite sea surface temperature (SST) increases on a daily basis, therefore the observed SST values do not depend on the geographical position but rather on the sampling date. Thus, although surface temperature is considered as one of the main factors influencing marine organisms, it cannot be used to characterize these hydrographic scenarios.

Chlorophyll-*a* concentrations at the surface were obtained from MODIS Aqua (or Moderate Resolution Imaging Spectro-radiometer aboard the Aqua satellite) mapped products, with 8 day and 4 km resolution [14,29]. For summer 2001, we used data provided by CERSAT (French ERS Processing and Archiving Facility), a daily analysis product of merged MODIS, MERIS and SeaWiFS data [18].

The regional climatic index IDEA characterizes the presence or absence of WIW in the Balearic channels through the use of winter air temperature anomalies in the Gulf of Lions [28]. This index is defined as a standardized air temperature anomaly, T_s:

$$T_s = \frac{T - \overline{T}}{\sqrt{\overline{\left(T - \overline{T}\right)^2}}}$$

(1)

where T is the mean winter surface air temperature at a point close to the Gulf of Lions (42.5 °N, 5.0 °E) for each year, and the overbar indicates temporal average during the winter months over the 1949-2004 period [28]. For the present study we used daily air surface temperature (1000 hPa) from 1948 to present from the NCEP/NCAR Reanalysis database [20].

Other data used in this study were obtained in the course of various projects developed by the Spanish Institute of Oceanography (IEO) and are compiled under the IBAMar database [4] accessible under request. The spatial coverage extends from the Alboran Sea to Cape Creus, including the Balearic Islands. The period used in this study expands from 1985 to 2012 and data correspond to projects BALEARES, IBIZA, CANALES, CIRBAL and RADMED [3], which were developed within the area using similar strategy and methodology for data collection. The detailed list of data used is shown in table 3. A reference is provided when the data correspond to other projects not compiled under the IBAMar data base.

3. Results

3.1. Hydrographical scenarios

Figure 2 shows the Map of Absolute Dynamic Topography for June 2001 to 2005 and 2012 calculated from the MSLA provided by AVISO and the deduced geostrophic currents. The dates have been chosen to be coincident with the surveys (Table 2) except for 2003 when the survey was in July. Figure 3 shows the dynamic height at 35 m, calculated from the CTD data and interpolated on the regular grid, and the deduced geostrophic currents for each Tunibal survey.

Dynamic height and deduced geostrophic currents can be considered synoptic during the sampling period because the satellite MADT main structures and its deduced currents show no significant changes during the duration of the surveys (Fig. 2 and similar for previous and posterior weeks not shown). Therefore the seasonal heating is homogeneous in the area of study and does not modify significantly the mesoescalar structures during the sampling period. Salinity maps are useful to detect salinity fronts as a proxy for the separation between recent AW and resident AW, and other mesoscale structures. Figure 4 shows the salinity measured by CTD at 35 m depth for each Tunibal survey. The boundary between recent and resident AW is marked in the figure with a black broken line. The same line derived from the salinity dsitribution is shown in the dynamic height (Fig. 3) to help the discussion.

The surface chlorophyll-*a* concentration maps will be used as a help to localize the density fronts since Chl-*a* fronts are very often related with the vertical velocities associated to oceanic fronts (Landry et al. 2012), surface Chl-*a* has been used to locate fronts due to the confluence of different water masses [43] and in the study area surface Chl-*a* seems to be highly related with resident AW in summer. Figure 5 shows the horizontal distribution of sea surface Chl-*a* concentration for June 2001 to 2005 and 2012 from MODIS Aqua. The dates have been chosen to be coincident with the surveys and to avoid cloud masks.

3.1.1. June 2001

In June 2001 the area was dominated by an input of fresh, newly advected AW spreading northwards through the Ibiza channel (Figs. 2A, 3A and 4A). In addition, a large bowl of AW ($S \le$ 37.2 at 35 m) is observed occupying the south-eastern region of Mallorca and south of Menorca (Fig. 4A). The northernmost area of the Balearic archipelago was occupied by resident AW. The confluence of the two AWs is detected as a salinity front separating the (northern) salty AW waters from the (southern) fresh AW. Associated to the front, an intense eastward geostrophic current ($\sim$ to 40 cm s^{-1}, Fig. 3A) run from the north of Ibiza to the south-east of Menorca, following a meandering anticyclonic/cyclonic path. In addition, three anticyclonic eddies were observed (at 38.5 °N, 2.5 °E, 38.5 °N, 4 °E, and at 39.5 °N, 4 °E -south of Menorca) carrying new AW towards the north of the region.

The areas with lower surface Chl-a concentration at the center of the domain (Fig. 5A) look to be related to areas of recent AW (Fig. 4A)

3.1.2. June 2002

Most of the area was occupied by resident AW (Fig. 4B). No transport of new AW was observed through the channels (Figs. 2B and 3B). Only some minor intrusions of new AW were observed between the islands of Cabrera and Menorca. The confluence of new and resident AW occurred at the southern border of the surveyed area ($\sim$ 38.5° N; Fig. 4B).

A small anticyclonic structure was observed south of Menorca (Fig. 3B). The areas with higher surface Chl-a concentration at the northwest of the domain, closer to the continental coast, (Fig. 5B) appear to correspond to areas of resident AW with S $>$ 38 (Fig. 4B)

3.1.3. July 2003

In July 2003 the Balearic archipelago was influenced by resident AW. The new AW was located to the south of Ibiza, and only minor intrusions of AW were observed at the Ibiza channel (Fig. 4C). In terms of mesoscale structures, a cyclonic circulation of resident AW was observed at the Mallorca channel (Fig. 3C and 4C), north of the front. Two intense anticyclonic gyres were detected south of the front and the current associated to the AW density front meanders along the 38.5 °N parallel (Fig. 3C). MADT (Fig. 2C) is plotted one month before the survey to allow for interannual comparison but main hydrographic structures described in figure 3C are already present in figure 2C. Surface Chl-a concentration (Fig. 5C) is plotted one week before the survey also to allow for interannual comparison. The areas with lower surface Chl-a concentration appear to correspond to the anticyclonic meanders of the current associated to the salinity driven density front (Fig. 2C), at the recent AW side.

3.1.4. June 2004

Resident AW occupied the western and northern part of the study area (Fig. 4D).

The most important hydrographical feature was the presence of mixed new and resident AW (37.4 $<$ S $<$ 37.5) south of Mallorca and Menorca Islands (i.e., at 39 °N, 3-5 °E; Fig. 4D). This structure was associated to currents (Fig. 3D), reinforcing an anticyclonic gyre south of Menorca. The areas with higher surface Chl-a concentration (Fig. 5D) look to be related to areas of resident AW with S $>$ 38 (Fig. 4D)

3.1.5. June 2005

New AW occupied the southwestern part of the study area, including the Ibiza and Mallorca channels (Fig. 4E). An anticyclonic eddy, formed by fresh AW centered at 38.5 $^\circ$N, 2.5° E, was found south the Mallorca channel (Figs. 3E and 4E). The front separating new and resident AW meanders between Ibiza and Mallorca, returning into the Algerian basin through the Mallorca channel (Figs. 2E and 3E). Resident AW was observed to the eastern part of the domain. A weak anticyclonic eddy was located to the south of Menorca Island. The areas with higher surface Chl-*a* concentration at the northwest of the domain, closer to the continental coast, (Fig. 5E) correspond with areas of resident AW with S $>$ 38 (Fig. 4A) and minimum values correspond to areas of new AW.

3.1.6. June 2012

The area was entirely occupied by resident AW (Fig. 4F). The salinity front separating new and resident AW (S $\approx$ 37.5) was found to the southern limit of the domain (Fig. 4F). The northern boundary of the front was associated to a northeastward geostrophic current running from the south of Ibiza to the south of Menorca, describing a meandering anticyclonic/cyclonic path (Fig. 2F). An anticyclonic structure at 39 $^\circ$N, 3.5 $^\circ$E containing relatively fresh water was found south of Mallorca. This structure reinforced the anticyclonic gyre typically found to the south of Menorca (Fig. 2F). The areas with higher surface Chl-*a* concentration at the northwest of the domain, closer to the continental coast, (Fig. 5F) correspond with areas of resident AW with S $>$ 38 (Fig. 4A).

3.2. Presence/absence of WIW at the Balearic channels

Five strategic locations were chosen to characterize the hydrographic properties of intermediate water masses around the study area (Fig. 1B). Two stations are located at the Ibiza and Mallorca channel, respectively. Two stations are deep stations at the north of Menorca and close to Cabrera Island. The fifth station is located north of Mallorca, to characterize the water masses properties of the Balearic Current.
Figure 6 shows the θ-S diagram for each Tunibal survey at the five selected stations. Local values for the different water masses are shown as boxes enclosing their corresponding core ranges. WIW is detected in a θ-S diagram bya relative minimum in temperature ($\theta < 13^\circ$C, Table 1) at intermediate water depths (from 100 to 300 m). According to Tunibal surveys, in 2001 and 2005 WIW was not found in the channels (Fig. 6A and E). In 2002 and 2004, WIW was found in the Ibiza channel (Fig. 6B and D), while in 2003 WIW was observed in the Mallorca channel (Fig. 6C). In 2012, there was WIW with salinity values slightly higher than usual ($\sim$ 38.32) (Fig. 6F). Contemporary surveys (e.g. RADMED-0312, Table 3) corroborate the presence of WIW in the channels in spring 2012. Local salinity values in 2012 were slightly higher than usual on the whole water column, including those corresponding to LIW (Fig. 6F).

4. Discussion

4.1. On the position of the front in presence/absence of WIW in the channels

The results presented above allow to outline, in a first order approach, the following situations:
(i) If there is WIW at the channels
the new AW do not progress northwards through the Ibiza channel in June, and deviates along

the south of Ibiza and Formentera towards Mallorca Island. The oceanic density front that separates new AW (coming from the south) and resident AW (coming from the north) is located at that time south of the islands or along the Emil Boudot escarpment (approximately along the 1000 m bathymetric line). This pattern was observed around June 2002, 2004 and 2012 and July 2003 (Figs. 2 and 3).

(ii) If WIW is not blocking the Ibiza channel, in June new AW progresses northwards, surrounding the west slope of Ibiza and usually crossing the Mallorca channel towards Cabrera Island. Under these circumstances the oceanic density fronts in June appear north of 39 °N. This pattern was observed in June 2001 and 2005.

In both cases, (i) and (ii), geostrophic currents associated to the new/resident AW front form meanders and gyres that allow intrusions of new AW towards higher latitudes (see e.g., years 2003, 2004, 2005, 2012 in Figs. 3 and 4).

This sketch for recent AW circulation at the beginning of the summer is in general agreement with [33] observations and [32] model results. The WIW produces a downward tilting of isopycnals and the anticyclonic structure is observed in some cases to be coherent from the surface down to 800 m [33]. [32] model shows that when there is WIW accumulated at the north of the Ibiza channel the anticyclonic gyres, "weddies", may block the Northern Current, which is partly redirected toward the Balearic slope. In this case the new AW input cross the Ibiza channel after 50 days of model run to reinforce the Balearic Current. The model also shows that when there is no WIW the Northern Current flows southward close to the continental slope and the recent AW flows northward through the Ibiza Channel since the first day of model run.

Tunibal surveys show that there is a good correspondence between the presence/absence of WIW in the channels and the meridional position of the oceanic front separating new AW from resident AW at the beginning of the summer.

4.2. On the use of the IDEA index to forecast the presence/absence WIW in the channels

WIW is formed in winter, in the northwestern Mediterranean and along the continental slope of the Iberian Peninsula [45].

The IDEA index states that in mild winters ($Ts>1$), little WIW is formed, so the lenses of WIW can flow through the Ibiza channel. In contrast, in cold winters ($Ts<1$), a larger amount of WIW reaching the channels can effectively block them in the following spring. Values of Ts between 0.5 and 1.0 would suggest some uncertainty [28].

Figure 7 shows the mesoscale IDEA index and the presence/absence of WIW in the channels from 1985 to 2012 according to Tunibal (2001-2005 and 2012) and other in-situ surveys (Table 3) obtained from the IEO monitoring program and compiled under the IBAMAR database or other published results. There is good agreement between the presence of WIW in the channels and the IDEA index. In particular, for the Tunibal surveys, the in-situ results (Fig. 6) show absence of WIW in the channels for year 2001, while presence of WIW in 2002, 2003, 2004 and 2012. Considering historical surveys from 1985 to present (Table 3) the IDEA index represents very well the presence/absence of WIW in the channels, as already shown by [28] until year 2004.

From a hydrographic point of view, 2005 was an unusual year. Episodes of extremely severe cold winter conditions lead to violent convective events, involving the formation of a thermohaline anomaly in the WMDW [23]. The deep water (DW) thermohaline anomaly can be observed in the 2005 $\theta - S$ diagram in figure 6E as a "hook" within the DW box at the deep stations of Menorca and Cabrera. Such strong cold convective circumstances lead to the formation of large amounts of new WMDW [13] at the cost of less WIW formation. This

would explain the disagreement between the absence of WIW in the channels during 2005 spring with the IDEA index for 2005. Moreover, it also indicates the need to extend the IDEA index to account for both WIW and WMDW formation or to use it with care if there are extreme climatological circumstances.

According to our observations it is possible to use a regional climatic index to forecast in most of the cases the presence of WIW in the channels, which in turn, determines the meridional location of the new AW oceanic front at the beginning of thesummer. The possibility of forecasting the position of the new AW oceanic front is expected to help to answer some biological questions.

4.3. On the position of the oceanic front and its biological implications

Satellite-derived surface Chl-*a* and sea surface temperature have been used for detection of oceanic fronts (e.g. [43,41]). In the area of study it gives the impresion that surface Chl-*a* concentration in summer is higher over resident AW. This could be due to the nutrient input from continental river discharge [10] that would affect more to the resident AW, that has followed a complete cyclonic path around the western Mediterranean basin, than to the recent AW, just arrived into the Mediterranean. A detailed quantitative analysis of the surface Chl-*a* together with the CTD available data would help to clarify the effectiveness of remote sensed data on the detection ofthe oceanic front around the Balearic islands.

One aspect typical from the mesoscale structures is the vertical motion which in the area of study could be linked to the biomass of mesopelagic fish [9] and may also influence the size structure of phytoplankton [39]. The main frontal areas could enhance the productivity of the lower trophic levels [35,22]

The hydrographic data presented in this work has been used in previous studies to explain the timing and the location of the spawning of Atlantic Bluefin tuna (ABT), whose spawning distribution in the area is related to the distribution of fresh AW and the location of the oceanic front separating new AW from resident AW [16,1,2]. The AW oceanic front position is also important for the spatial overlapping among different sizes of fish larvae [44], which enhance the survival of other species, e.g. piscivorous tuna larvae [37].

In addition, a quasi-permanent anticyclonic gyre was observed to the south of Menorca in all Tunibal surveys. This area seems to be a retention zone for meroplankton [2], and the location of the gyre could be used as a signal to predict the spawning distribution of several species, e.g. albacore tuna [37].

4.4. On the biological implications of predicting frontal positions using the IDEA index

Many studies have successfully correlated variations in abundances of marine organisms with the hydrographic/climatic environment (e.g. [30]). However, most studies do not provide a mechanical explanation to their observations. Some authors have shown the need of a process-based perspective, in which a climatic index is used to interpret ecosystem changes based on the species phenology (e.g. [21]). The hydrographic scenarios derived from our analysis could enable a connection between climate, regional oceanography and the life history traits of marine organisms.

The possibility of using the IDEA regional climatic index to forecast the meridional position of the AW oceanic front opens new boundaries of exploration.

The IDEA index could also be used to further understand the connectivity of marine populations. The connectivity (i.e., the passive dispersal of early live stages of fish) between populations of pelagic and some coastal species is related to oceanographic processes that drive

dispersal, typically at surface water masses (e.g. [42]). For some demersal species whose spawning occurs in intermediate waters, connectivity could be determined by the link between those intermediate water masses and surface waters where the eggs finally stand. Once larvae hatch they will depend on the horizontal advection of the surface layer, which ultimately determines recruitment areas. This is the case of the European hake [19], for which the recruitment area around the Islands depends on the origin of the eggs (i.e., if they are originally laid down near the mainland, or near the Islands). Since the IDEA index allows to link WIW to frontal AW dynamics, it could be used to further explore the connectivity of marine populations between the mainland and the Islands.

Therefore, our results offer a challenge for short-term forecasting in the view of the ecosystem-approach and spatial based management. Once the relationships among a given species and environmental scenarios have been established, one could take advantage of climatic models to obtain the probabilistic distribution of larvae. Models could also be used to examine the probable evolution of meroplanktonic groups under different future environmental scenarios and evaluate potential consequences in the ecosystem functioning.

5. Conclusions

The presence/absence of WIW in the channels determines the meridional position of the oceanic density front between new and resident AWs at the beginning of the summer. In a first order approximation, when WIW is present in the Ibiza channel the new AW cannot move northwards across the channel in June. In this case the oceanic density front appears either at the south of the islands or along the Emil Boudot escarpment. If WIW is not present in the channels, new AW progresses northwards crossing the Ibiza channel along the insular slope, surrounding the north of Ibiza, and usually crossing the Mallorca channel. In the latter case, the oceanic density front is closer to the Balearic Islands.

In the area of study surface Chl-*a* concentration in summer seems to be higher over resident AW. A detailed quantitative analysis of the surface Chl-*a* together with the CTD available data is necessary to clarify the effectiveness ofremote sensed data on the detection of the oceanic front around the Balearic islands.

A quasi-permanent anticyclonic gyre, that acts as a retention zone for some meroplanktonic organisms [2], was observed to the south of Menorca in all Tunibal surveys.

A good correspondence exists between the regional climatic index IDEA and the presence of WIW at the Balearic channels [28]. The relation of the presence/absence of WIW with the meridional position of the oceanic front allows to use the IDEA index, in a first order approximation, to characterize the position of the oceanic front.

Understanding ecosystems dynamics is a challenge for short-term forecasting in the framework of ecosystem-approach and spatial based management [21]. Our results would allow a straightforward connection between atmospheric forcing, regional oceanography and fish phenology and could be an important contribution to the understanding of regional marine ecosystem dynamics. Extending this experiment to include the use of numerical forecasting models is expected to have relevant implications for ecosystem management strategies.

Acknowledgments

References

[1] Alemany, F., Deudero, S., Morales-Nin, B., López-Jurado, J.L., Jansà, J., Palmer, M., Palomera, I., 2006. Influence of physical environmental factors on the composition and horizontal distribution of summer larval fish assemblages off mallorca island (balearic archipelago, western mediterranean). Journal of Plankton Research 28, 473–487.

[2] Alemany, F., Quintanilla, L., Velez-Belchí, P., García, A., Cortés, D., Rodríguez, J.M., Fernández de Puelles, M.L., González-Pola, C., López-Jurado, J.L., 2010. Characterization of the spawning habitat of Atlantic bluefin tuna and related species in the Balearic Sea (western Mediterranean). Progress in Oceanography 86, 21–38.

[3] Amengual, T., Aparicio, A., Balbín, R., Fernández de Puelles, M., García-Martínez, M., Gaza, M., Jansá, J., Lopez-Jurado, J., Morillas, A., Moya, F., Plaza, F., Serra, M., Tel, E., Vargas-Yáñez, M., Vicente, L., Zunino, P., Álvarez, M., Bange, H., 2010. Implementing a multidisciplinary monitoring system in the Spanish Mediterranean, in: 39th CIESM, CIESM The Mediterranean Science Commision, Venecia.

[4] Aparicio, A., López-Jurado, J., Balbín, R., Jansá, J., Amengual, B., 2012. IBAMar 2.0: 36 years sampling on the Western Mediterranean Sea, in: EGU General Assembly Conference Abstracts, p. 8476.

[5] Astraldi, M., Gasparini, G., 1992. The seasonal characteristics of the circulation in the north mediterranean basin and their relationship with the atmospheric-climatic conditions. Journal of Geophysical Research 97, 9531–9540.

[6] Aviso, 2012. MADT user manual, 2012. http://www.aviso.oceanobs.com/fileadmin/documents/data/tools/hdbk_duacs.pdf.

[7] Bahurel, P., Adragna, F., Bell, M., Jacq, F., Johannessen, J., Le Traon, P., Pinardi, N., She, J., 2009. Ocean Monitoring and Forecasting Core Services: The European MyOcean Example. Technical Report. MyOcean.

[8] Bakun, A., 2006. Fronts and eddies as key structures in the habitat of marine fish larvae: opportunity, adaptive response and competitive advantage. Scientia Marina 70, 105–122.

[9] Balbín, R., Flexas, M., López-Jurado, J., Peña, M., Amores, A., Alemany, F., 2012. Vertical velocities and biological consequences at a front detected at the Balearic Sea. Continental Shelf Research 47, 28–41.

[10] Bethoux, J., 1989. Oxygen consumption, new production, vertical advection and environmental evolution in the Mediterranean Sea. Deep Sea Research Part A. Oceanographic Research Papers 36, 769–781.

[11] Bretherton, F., Davis, R., Fandry, C., 1976. A technique for objective analysis and design of oceanographic experiments applied to MODE-73, in: Deep Sea Research and Oceanographic Abstracts, Elsevier. pp. 559–582.

[12] Canals, M., Puig, P., de Madron, X., Heussner, S., Palanques, A., Fabres, J., 2006. Flushing submarine canyons. Nature 444, 354–357.

[13] CIESM, 2009. Dynamics of Mediterranean deep waters, in: CIESM Workshop Monographs, Malta.

[14] Feldman, G.C., McClain, C.R., 2012. Ocean Color Web. http://oceandata.sci.gsfc.nasa.gov/.

[15] Font, J., Salat, J., Tintoré, J., 1988. Permanent features of the circulation in the Catalan Sea. Oceanol. Acta 9, 51–57.

[16] García, A., Alemany, F., Velez-Belchí, P., Jurado, J.L., Cortés, D., de la Serna, J., Pola, C.G., Rodríguez, J., Jansá, J., Ramírez1, T., 2005. Characterization of the bluefin tuna spawning habitat off the Balearic Archipelago in relation to key hydrographic features and associated environmental conditions. Col. Vol. Sci. Pap. ICCAT 58, 535–549.

[17] García-Ladona, E., Castellón, A., Font, J., Tintoré, J., 1996. The Balearic current and volume transports in the Balearic basin. Oceanol. Acta 19, 489–497.

[18] Gohin, F., Druon, J., Lampert, L., 2002. A five channel chlorophyll concentration algorithm applied to seawifs data processed by seadas in coastal waters. International Journal of Remote Sensing 23, 1639–1661.

[19] Hidalgo, M., Tomás, J., Moranta, J., Morales-Nin, B., 2009. Intra-annual recruitment events of a shelf species around an island system in the NW Mediterranean. Estuarine, Coastal and Shelf Science 83, 227–238.

[20] Kalnay, E., Kanamits, M., Kistler, R., Collins, W., Deaven, D., Gandin, L., Iredell, M., Saha, S., White, G., Woollen, J., Zhu, Y., Leetmaa, A., Reynolds, R., Chelliah, M., Ebisuzaki, W., W.Higgins, Janowiak, J., Mo, K.C., Ropelewski, C., Wang, J., Jenne, R., Joseph, D., 1996. The ncep/ncar 40-year reanalysis project. Bulletin of the American Meteorological Society .

[21] Kleidon, A., Mooney, H.A., 2000. A global distribution of biodiversity inferred from climatic constraints: results from a process-based modelling study. Global Change Biology 6, 507–523.

[22] Landry, M., Ohman, M., Goericke, R., Stukel, M., Barbeau, K., Bundy, R., Kahru, M., 2012. Pelagic community responses to a deep-water front in the California Current Ecosystem: overview of the A-Front study. Journal of Plankton Research 34, 739–748.

[23] López-Jurado, J.L., González-Pola, C., Vélez-Belchí, P., 2005. Observation of an abrupt disruption of the long-term warming trend at the Balearic Sea, western Mediterranean Sea, in summer 2005. Geophysical Research Letters 32.

[24] López-Jurado, J.L., Marcos, M., Monserrat, S., 2008. Hydrographic conditions affecting two fishing grounds of Mallorca island (Western Mediterranean): during the IDEA Project (2003-2004). Journal of Marine Systems 71, 303–315.

[25] MEDAR-Group, 2002. MEDATLAS 2002 Mediterranean and Black Sea database of temperature, salinity and biochemical parameters climatological atlas, 4 CD-ROM., European Commission Marine Science and Technology Programme (MAST). IFREMER.

[26] MEDOC-Group, 1970. Observation of formation of deep water in the Mediterranean Sea. Nature 227, 1040.

[27] Millot, C., 1985. Some features of the algerian current. Journal of Geophysical Research 90, 7169–7176.

[28] Monserrat, S., López-Jurado, J.L., Marcos, M., 2008. A mesoscale index to describe the regional circulation around the balearic islands. Journal of Marine Systems 71, 413–420.

[29] OceanColor, 2011. Chlorophyll operational algorithm. http://oceancolor.gsfc.nasa.gov/ANALYSIS/ocv6/.

[30] Ottersen, G., Alheit, J., Drinkwater, K., Friedland, K., Hagen, E., Stenseth, N.C., 2005. Marine Ecosystems and Climate Variation. Oxford University Press. chapter The Responses of Fish Populations to Ocean Climate Fluctuations.

[31] Perkins, H., Pistek, P., 1990. Circulation in the Algerian basin during June 1986. Technical Report. DTIC Document.

[32] Pinot, J., Álvarez, A., Fernández, V., Riera, M., 1999. The role of winter intermediate waters in the spring-summer circulation of the balearic sea 2. a sensitivity numerical study. Journal of geophysical research 104, 29865–29.

[33] Pinot, J., Ganachaud, A., 1999. The role of winter intermediate waters in the spring-summer circulation of the Balearic Sea. I- Hydrography and inverse box modeling. Journal of geophysical research 104, 29.

[34] Pinot, J.M., López-Jurado, J.L., Riera, M., 2002. The CANALES experiment (1996-1998). Interannual, seasonal, and mesoscale variability of the circulation in the Balearic Channels. Progress In Oceanography 55, 335 – 370.

[35] Pinot, J.M., Tintoré, J., López-Jurado, J.L., de Puelles, M.L.F., Jansá, J., 1995.

Three-dimensional circulation of a mesoscale eddy/front system and its biological implications. Oceanol. Acta 18, 389–400.

[36]   Puig, P., de Madron, X.D., Salat, J., Schroeder, K., Martín, J., Karageorgis, A.P., Palanques, A., Roullier, F., Lopez-Jurado, J.L., Emelianov, M., Moutin, T., Houpert, L., 2013. Thick bottom nepheloid layers in the western Mediterranean generated by deep dense shelf water cascading. Progress in Oceanography 111, 1–23.

[37]   Reglero, P., Ciannelli, L., Alvarez-Berastegui, D., Balbín, R., López-Jurado, J., Alemany, F., 2012. Geographically and environmentally driven spawning distributions of tuna species in the western Mediterranean Sea. Marine Ecology Progress Series 463, 273–284.

[38]   Rio, M., Poulain, P., Pascual, A., Mauri, E., Larnicol, G., Santoleri, R., 2007. A mean dynamic topography of the mediterranean sea computed from altimetric data, in-situ measurements and a general circulation model. Journal of Marine Systems 65, 484–508.

[39]   Rodriguez, J., Tintoré, J., Allen, J., Blanco, J., 2001. Mesoscale vertical motion and the size structure of phytoplankton in the ocean. Nature 410, 360–363.

[40]   Salat, J., 1995. The interaction between the Catalan and Balearic currents in the southern Catalan Sea. Oceanologica acta 18, 227–234.

[41]   Saraceno, M., Provost, C., Piola, A.R., 2005. On the relationship between satellite-retrieved surface temperature fronts and chlorophyll a in the western south atlantic. Journal of Geophysical Research: Oceans (1978–2012) 110.

[42]   Schunter, C., Carreras-Carbonell, J., Macpherson, E., Tintoré, J., Vidal-Vijande, E., Pascual, A., Guidetti, P., Pascual, M., 2011. Matching genetics with oceanography: directional gene flow in a mediterranean fish species. Molecular Ecology 20, 5167–5181.

[43]   Takahashi, W., Kawamura, H., 2005. Detection method of the kuroshio front using the satellite-derived chlorophyll-a images. Remote Sensing of Environment 97, 83 – 91.

[44]   Torres, A., Reglero, P., Balbín, R., Urtizberea, A., Alemany, F., 2011. Coexistence of larvae of tuna species and other fish in the surface mixed layer in the NW Mediterranean. Journal of Plankton Research 33, 1793–1812.

[45]   Vargas-Yáñez, M., Zunino, P., Schroeder, K., López-Jurado, J., Plaza, F., Serra, M., Castro, C., García-Martínez, M., Moya, F., Salat, J., 2012. Extreme Western Intermediate Water formation in winter 2010. Journal of Marine Systems 105-108, 52–59.

Water mass	Values at origin	Local values
AW	$15.0 < \theta < 18.0$	$15.0 < \theta < 28.0$
	$36.15 < S < 36.50$	$36.50 < S < 37.50$
Resident AW	$13.0 < \theta < 28.0$	$13.0 < \theta < 28.0$
	$37.50 < S < 38.30$	$37.50 < S < 38.20$
WIW	$12.5 < \theta < 13.0$	$12.5 < \theta < 13.0$
	$37.90 < S < 38.30$	$37.90 < S < 38.30$
LIW	$14.0 < \theta < 15.0$	$13.0 < \theta < 13.4$
	$38.70 < S < 38.80$	$38.45 < S < 38.60$
WMDW	$12.7 < \theta < 12.9$	$12.7 < \theta < 12.9$
	$38.40 < S < 38.48$	$38.40 < S < 38.48$

Table 1. Potential temperature (θ) and Salinity (S) ranges of the different water masses in the area of study. AW=Atlantic Water. WIW: Western Mediterranean Intermediate Water. LIW: Levantine Intermediate Water. WMDW: Western Mediterranean Deep Water.

Survey	Dates (from - to)	number of CTD stations
Tunibal 0601	16/06/2001 - 09/07/2001	150
Tunibal 0602	07/06/2002 - 30/06/2002	193
Tunibal 0703	03/07/2003 - 30/07/2003	212
Tunibal 0604	17/06/2004 - 10/07/2004	190
Tunibal 0605	27/06/2005 - 23/07/2005	190
Atame 0612	21/06/2012 - 14/07/2012	178

Table 2. Summary of Tunibal surveys.

Presence/absence of WIW in the Balearic Channels

Year	WIW	Survey (MMYY)
1985	YES	BALEARES (0785 and 1085)
1986	YES	In Algerian Subbasin [31]

1987 YES BALEARES (0387 and 0587)
1988 YES BALEARES (0488 and 0688)
1989 YES FE 89 [17]
1990 NO MEDATLAS [25]
1991 YES IBIZA (0391 and 0791)
1992 YES IBIZA (0692 and 0792)
1993 YES IBIZA (0393, 0593 and 0693
1994 ?? No references
1995 YES MEDATLAS [25]
1996 YES CANALES (0496, 0596, 0696 and 0796)
1997 NO CANALES (0497, 0597, 0697 0897 and 1097)
1998 NO CANALES (0198, 0498 and 0698)
1999 YES CANALES (0599)
2000 YES HERCULE (0500) and CIRBAL (0900)
2001 NO TUNIBAL (0601) and CIRBAL (0301, 0501, 0601 and 1101)
2002 YES TUNIBAL (0602) and CIRBAL (0302 and 0502)e
2003 YES TUNIBAL (0703) and CIRBAL (0503)
2004 YES TUNIBAL (0604), CIRBAL (0404), IDEA (0404 and 0604)
2005 NO TUNIBAL (0605) and CIRBAL (0605 and 0905)
2006 YES CIRBAL (0406 and 0606)
2007 NO RADMED (0707, 1007)
2008 YES RADMED (0211, 0511, 0711)

2009	YES	RADMED (0309, 0509, 0709)
2010	YES	RADMED (0210, 0410, 0710, 1110)
2011	YES	RADMED (0211, 0511, 0711)
2012	YES	ATAME (0607) and RADMED (0312)

Table 3. Presence/absence of WIW in the channels according to hydrographical surveys conducted by IEO, and included in the IBAMar database, or other published surveys.

Figure 1. (A) Western Mediterranean Sea and main currents characterizing the regional circulation. The Algerian, Northern and Balearic currents are shown as dark thick arrows and the Algerian gyres are indicated as light dotted arrows. Light grey lines denote isobaths (100 m, 500 m, 1000 m, and 2000 m). (B) Station distribution used during Atame-0612 as an example of Tunibal standard grid station planning. Main geographical features are sown for reference. Circles (colored in the online version) indicate strategic stations used to characterize intermediate-depth water masses around the Islands (see Fig. 6).

Figure 2. Map of Absolute Dynamic Topography (dynamic cm) obtained from altimetry data and deduced geostrophic currents for the dates coincident with each Tunibal survey (except for the 2003 survey when SSH is represented at the end of June, one month before the survey). (A) 2001, (B) 2002, (C) 2003, (D) 2004, (E) 2005, (F) 2012.

Figure 3. Dynamic height (DH, in dynamic cm) interpolated maps and deduced geostrophic currents for each Tunibal survey. Values of DH at every CTD station are shown in circles. The boundary between new/resident AW obtained from the salinity maps is marked with a black broken line. (A) 2001, (B) 2002, (C) 2003, (D) 2004, (E) 2005, (F) 2012.

Figure 4. Salinity interpolated maps and values at every CTD station (in circles) for each Tunibal survey. The boundary between new/resident AW is marked with a black broken line. (A) 2001, (B) 2002, (C) 2003, (D) 2004, (E) 2005, (F) 2012.

Figure 5. Horizontal distribution of surface chlorophyll-a concentration in the Balearic region at the end of June for years 2002 to 2005 and 2012 (except for 2002 when there is no data available before the 7th of July). (A) 2001, (B) 2002,(C) 2003, (D) 2004, (E) 2005, (F) 2012.

Figure 6. Potential temperature (θ) versus Salinity (S) diagram for each Tunibal survey. Lines (colored in the online version) correspond to five selected stations (Fig. 1) at: Ibiza Channel (black line), Mallorca channel (dotted light gray or red in the online version), Cabrera Island (dotted dark gray or blue in the online version), North of Menorca (gray line or pink in the online version), and north of Mallorca (thick gray line or green in the online version). Local values for WIW, LIW and DWs of Table 1 are shown as boxes that enclose their corresponding core ranges. (A) 2001, (B) 2002, (C) 2003, (D) 2004, (E) 2005, (F) 2012.

Figure 7. The IDEA index from 1985 to 2012. Dots indicate the presence(white dots)/absence(black dots) of WIW according to Tunibal surveys, IBAMAR data base and other published results. Surveys are detailed in Table 3.
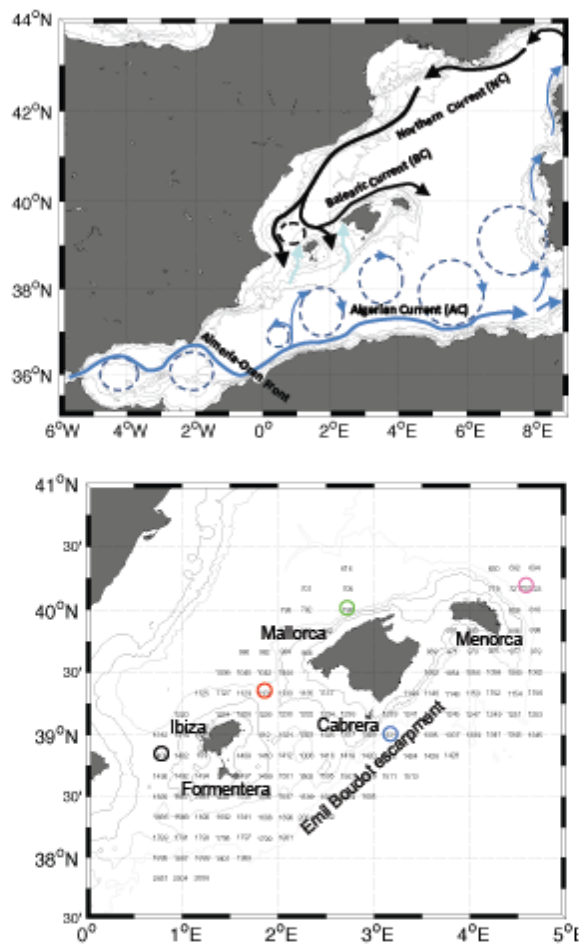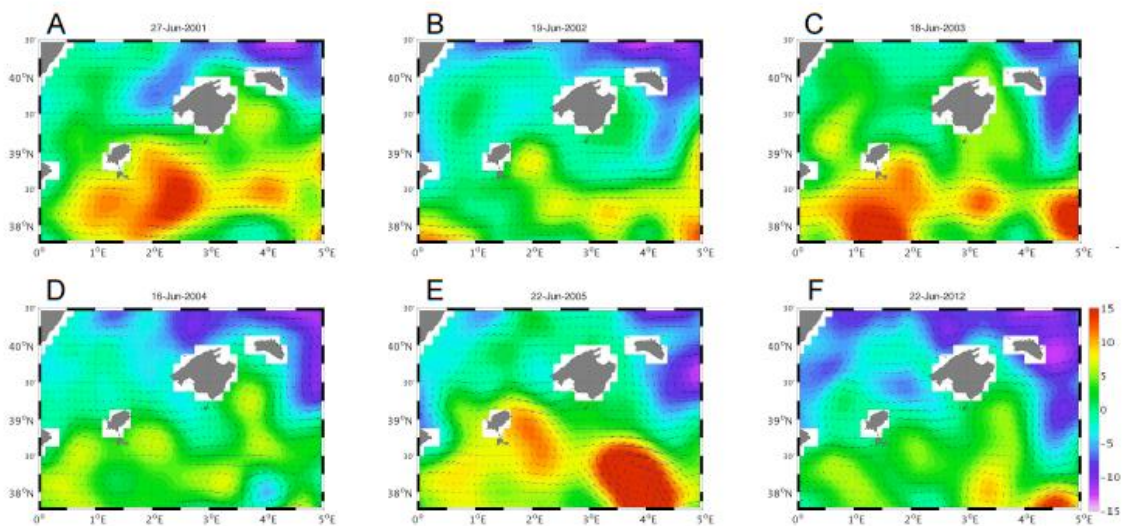
Figure 1: (A) Western Mediterranean Sea and main currents characterizing the regional circulation. The Algerian, Northern and Balearic currents are shown as dark thick arrows and the Algerian gyres are indicated as light dotted arrows. Light grey lines denote isobaths (100 m, 500 m, 1000 m, and 2000 m). (B) Station distribution used during Atame-0612 as an example of Tunibal standard grid station planning. Main geographical features are sown for reference. Circles (colored in the online version) indicate strategic stations used to characterize intermediate-depth water masses around the Islands (see Fig. 6).

Figure 2: Map of Absolute Dynamic Topography (dynamic cm) obtained from altimetry data and deduced geostrophic currents for the dates coincident with each Tunibal survey (except for the 2003 survey when SSH is represented at the end of June, one month before the survey). (A) 2001, (B) 2002, (C) 2003, (D) 2004, (E) 2005, (F) 2012.
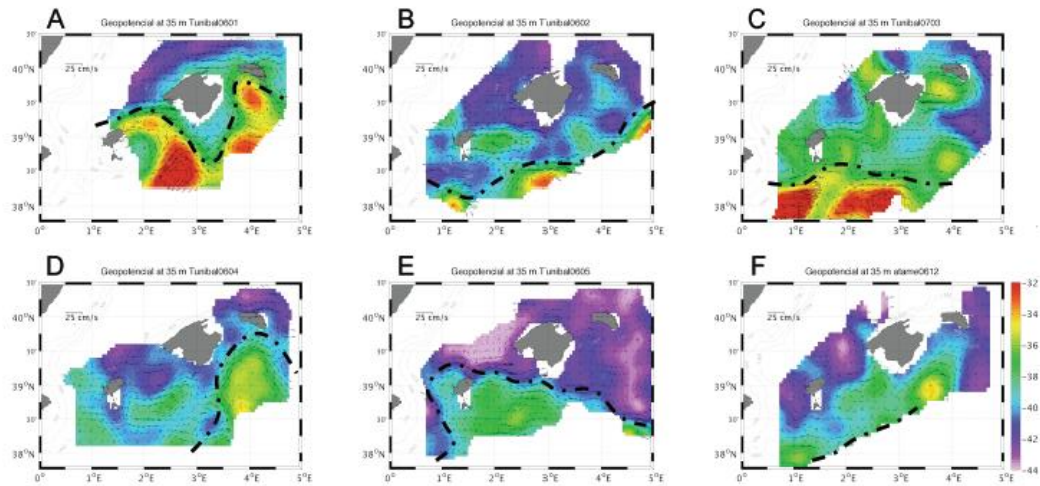
Figure 3: Dynamic height (DH, in dynamic cm) interpolated maps and deduced geostrophic currents for each Tunibal survey. Values of DH at every CTD station are shown in circles. The boundary between new/resident AW obtained from the salinity maps is marked with a black broken line. (A) 2001, (B) 2002, (C) 2003, (D) 2004, (E) 2005, (F) 2012.

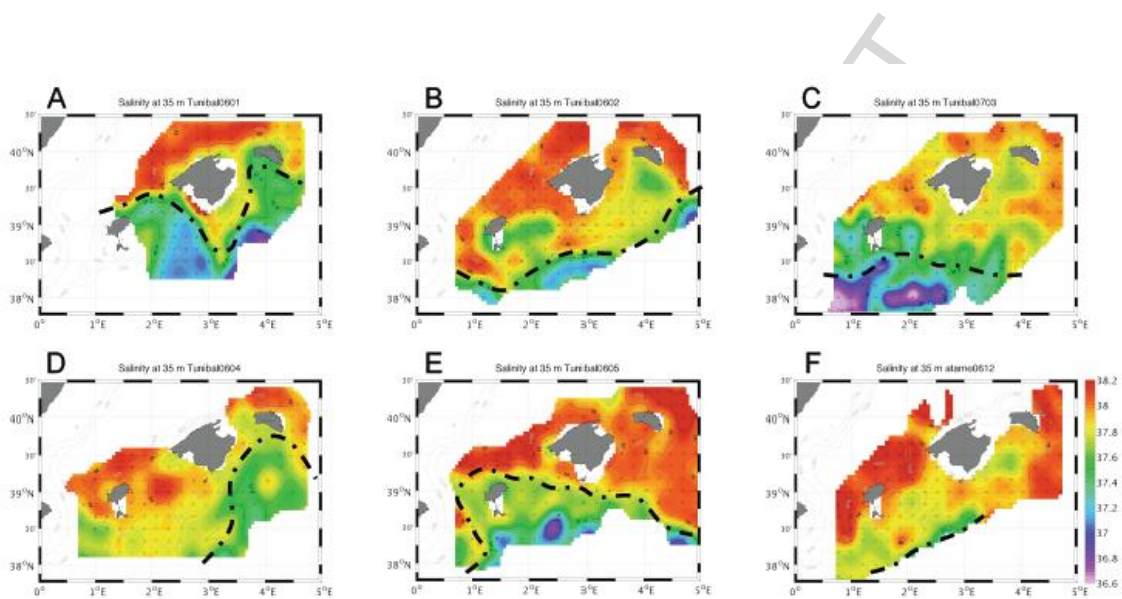Figure 4: Salinity interpolated maps and values at every CTD station (in circles) for each Tunibal survey. The boundary between new/resident AW is marked with a black broken line. (A) 2001, (B) 2002, (C) 2003, (D) 2004, (E) 2005, (F) 2012.
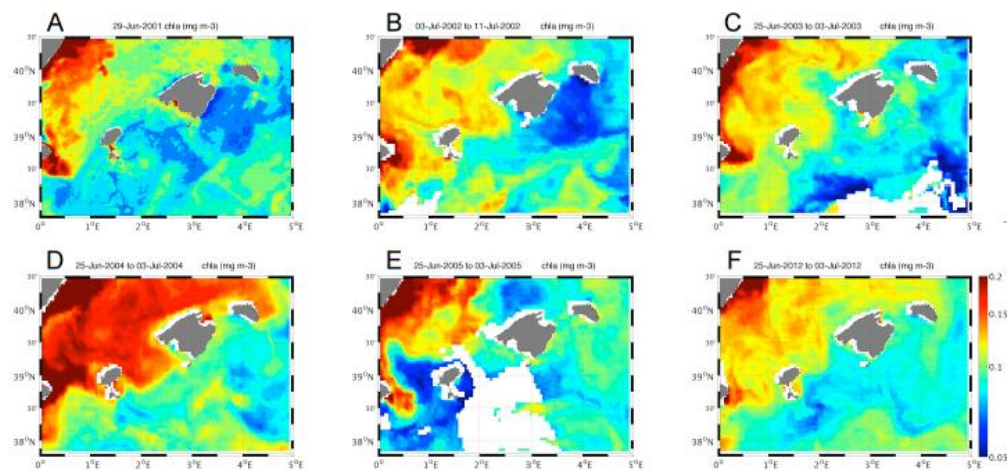
Figure 5: Horizontal distribution of surface chlorophyll-*a* concentration in the Balearic region at the end of June for years 2002 to 2005 and 2012 (except for 2002 when there is no data available before the 7th of July). (A) 2001, (B) 2002, (C) 2003, (D) 2004, (E) 2005, (F) 2012.
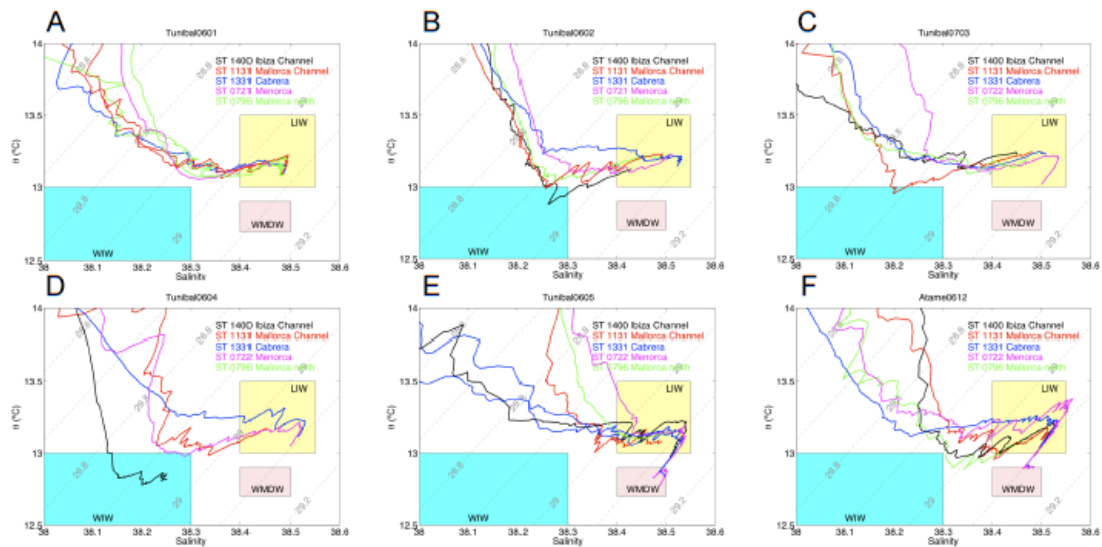
Figure 6: Potential temperature (θ) versus Salinity (S) diagram for each Tunibal survey. Lines (colored in the online version) correspond to five selected stations (Fig. 1) at: Ibiza Channel (black line), Mallorca channel (dotted light gray or red in the online version), Cabrera Island (dotted dark gray or blue in the online version), North of Menorca (gray line or pink in the online version), and north of Mallorca (thick gray line or green in the online version). Local values for WIW, LIW and DWs of Table 1 are shown as boxes that enclose their corresponding core ranges. (A) 2001, (B) 2002, (C) 2003, (D) 2004, (E) 2005, (F) 2012.
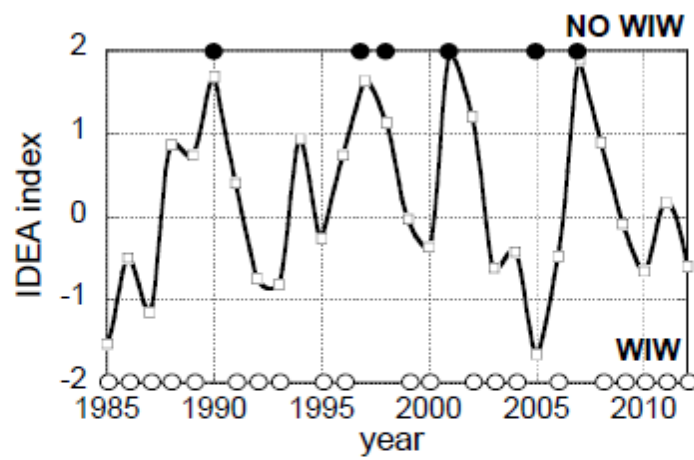
Figure 7: The IDEA index from 1985 to 2012. Dots indicate the presence(white dots)/absence(black dots) of WIW according to Tunibal surveys, IBAMAR data base and other published results. Surveys are detailed in Table 3.